Lasers in Manufacturing Conference 2023

Surface smoothening of thermal sprayed Hastelloy® C-276 coatings by laser polishing

N. Seiler[a,*], M. Hofele[a], M. Dauner[b], H. Riegel[a]

[a]*Aalen University, Beethovenstraße 1, 73430 Aalen, Germany*
[b] *Rybak + Hofmann rhv-Technik GmbH + Co. KG, Eisentalstraße 27, 71332 Waiblingen, Germany*

Abstract

Thermal sprayed coatings of the nickel-base alloy Hastelloy provide highly effective corrosion protection and thermal resistance. However, the sprayed surfaces exhibit a rough surface topography (Ra = 5.6 µm) with exposed porosity. In addition, thicker layers of material than necessary must be applied to compensate the material removal during mechanically surface finishing. This research work investigates the possibility of volume-preserving laser polishing to smoothening the rough surface structure of thermal sprayed Hastelloy C-276 coatings while closing the exposed porosity. In the future, laser remelting is expected to eliminate the material waste produced by conventional mechanical post-processing. Correlations between the laser parameters and the resulting coating layer properties such as roughness, residual surface structures are worked out enabling a relative roughness improvement of up to 81%. However, delamination and the formation of cracks occurs even at less energy density and created remelting depths, limiting the process ability.

Keywords: Laser remelting; post-processing; surface treatment; thermal spraying; flame spraying; high velocity flame spraying (HVOF); Hastelloy

1. Introduction

Thermal spraying is a coating process for metal surfaces. During this process the material in form of powder, is sprayed under high temperatures and pressure onto the surface of a workpiece. Powder particles melt inside of the flame and impinges onto the workpiece at speeds of approximately 600-700 m/s creating

* Corresponding author. Tel.: +49-7361-576-2663.
E-mail address: nathan.seiler@hs-aalen.de.

adhesion at the surface. Since, in contrast to other coating processes, there is no melt-metallurgical bonding, the material combinations that can be applied are almost unlimited, Herman et al., 2000.

Hastelloy® C-276 is a high performance alloy, which is based on nickel, chromium and molybdenum. It is known for its excellent properties in terms of resistance against corrosion and chemical attack, while being insensitive to temperature. Therefore, it is of ideal use in areas such as aerospace engineering, chemical processing and power generation, Singh et al., 2023.

However, thermal sprayed surfaces typically exhibit a rough surface texture and residual porosity, which prevents direct use in industrial applications, especially for functional surfaces with precise geometric requirements. Further the rough surface structure causes an increase of abrasion and wear. Due to the existing surface structure crevice corrosion can occur and reduces the corrosion resistance in harsh environmental conditions, Ni et al., 2009. Additional, exposed pores in the surface form a pathway for corrosion to the substrate, resulting in reduced durability and lifetime of the coated component, Huang et al., 2023.

Therefore, in conventional manufacturing thermal sprayed surface coatings usually require mechanical post-treatment, which needs the application of a thicker coating with an offset to compensate the material removal during mechanical subtractive post-treatment (e.g. machining or grinding), Srinath et al., 2022.

This work investigates the possibility to replace the currently necessary mechanical post-processing of thermal sprayed surface coatings by volume-preserving laser polishing in order to eliminate the unnecessary loss of material, smoothening the rough surface structure while simultaneously reducing the surface near porosity.

At laser polishing, a thin layer of the surface is molten by the laser beam. Within the melt pool, surface tension as well as capillary forces cause material to flow from the “mountains” (surface peaks) to the “valleys” (surface indentations). For areal treatment the laser beam is guided in overlapping hatchings over the surface. In order to stabilize the process and to generate a thin melt pool high scanning velocities are applied.

When treating metal coating by laser polishing, due to different thermal expansion coefficients between the substrate and the coating, internal stresses near the surface can occur as a result of local heating, remelting and subsequent cooling, which may lead to cracks or delamination of the coating, Bordatchev et al., 2014.

Within this study laser polishing of thermal sprayed Hastelloy® C-276 coatings is investigated. Hereto a process parameter study is performed by varying various laser parameters such as laser power, scan speed and hatch distance. Subsequently, the polished samples are investigated with respect to their coating properties by means of optical surface measurements and metallographic characterization with focus on the surface smoothness in relation to the initial state after thermal spraying.

2. Experimental design and analysis methodology

2.1. Material and specimen

The laser polishing experiments are performed on a Hastelloy® C-276 coating, which is sprayed by high velocity oxygen fuel (HVOF) onto rectangular plates of cold rolled S235JRC with dimensions of 100x100x5 mm. For the coating process the substrate surface is pre-treated by sand blasting to increase the surface roughness and therefore the layer connection. HVOF was applied using kerosene as energy source with a coating speed of 800 mm/s and a powder feed rate of 70 g/min. 40 layers were built up with a track spacing of 6 mm.

The chemical composition of the used Hastelloy® C-276 powder is presented in Table 1. The powder material from the manufacturer Oerlikon is gas atomized with an average particle size of < 55 µm and spherical shape (based on the manufacturer’s specifications).

Table 1. Chemical composition of the used Hastelloy® C-276 powder for thermal spraying

Element	Ni	Cr	Mo	W	Fe	Mn	V	C	Si	Al	Co	Ti	P	S	TAO
Content (wt.%)	58,4	15,8	15,8	4,5	4,3	0,6	0,14	0,06	0,1	< 0,1	< 0,1	< 0,1	0,008	0,001	< 0,1

2.2. Applied laser polishing setup

Laser polishing is performed using a near infrared disc laser TruDisk4002 of the manufacturer TRUMPF (max. laser power 4000 W, wavelength of 1030 nm). A 3D Scanner optic I-PFO-PO from TRUMPF with a focal length of 600 mm, resulting in a focal diameter of 870 µm, is used to focus and guiding the laser beam over the coating surface. The optic is mounted on a 6-axis robot, which is used for positioning the scanner over the treated polishing array.

Polishing fields with a size of 10x10 mm^2 are treated under inert gas atmosphere (argon 5.0) onto the coated samples in a modular process chamber, specially manufactured for laser polishing. The oxygen meter Zyrox SGM7 ensures, that the oxygen content during laser polishing is < 50 ppm. Each field is exposed bi-directionally and perpendicular to the coating process. A waiting time of 30 s is applied between the exposure of the individual polishing fields in order to ensure that a consistent base temperature prevails throughout the test series and to eliminate heat accumulation through the neighbouring test field.

The experimental setup, as well as a schematic representation of the specimen geometry and the laser polished fields are shown in Fig. 1.

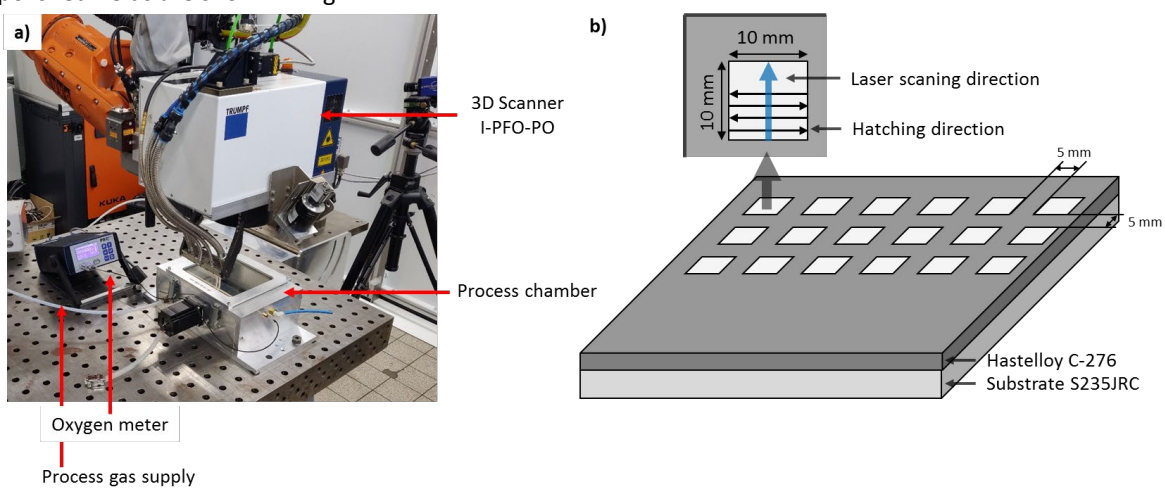

Fig. 1. (a) Experimental setup, (b) schematic representation of specimen geometry and laser polishing field size

Laser polishing was performed with the focal beam on the work peace surface. The laser source was used at the continuous laser operation mode. This work is divided into two test series. First, the influence of the laser beam intensity and energy per unit length onto the achievable surface quality is investigated. Second, the influence of the track overlap and the overall energy density is studied.

2.3. Used measurement devices and evaluation methods

The surface characteristic is analysed using the Carl Zeiss Axio Zoom.V16 light microscope at 8x and 100x magnification. For quantitative surface roughness analysation, the samples are measured using the

MarSurf M400 tactile perthometer. Here, the initial surface with Ra >> 2 µm are measured with a cut-off wavelength of 2500 µm, while at the polished surfaces the cut-off wavelength is set to 800 µm. Five linear measurements are made per specimen, evenly distributed over the surface and oriented at 90° to the scanning direction. The global topography within the polishing field is examined using the KEYENCE VX-X3050 3D laser scanning microscope with 5x magnification. The microstructure is analysed by means of a white light interferometer of type AMETEK NewView 8300 with a magnification of 10x. For the analysis of the porosity, the remelting zone a possible internal defects, metallographic cross sections perpendicular to the scanning direction are polished and imaged with the Carl Zeiss Axio Imager.Z2 Vario microscope at 200x magnification.

3. Results and Discussion

3.1. Initial surface characteristics

The thermally sprayed Hastelloy® coating surface has a homogeneous but rough surface topography. Fig. 2 shows the initial surface of the coated samples as well as the internal microstructure, in which pores are clearly visible.

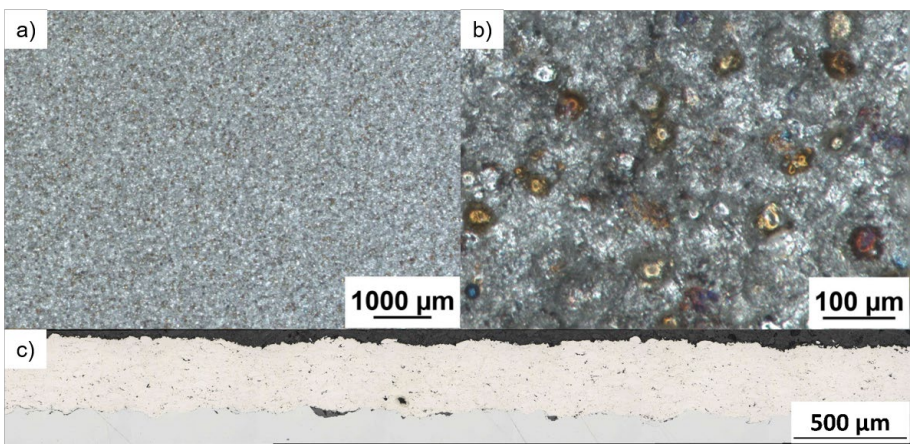

Fig. 2. Light microscope image of the initial surface structure after thermal spraying. a) 8x magnification and b) 100x magnification and of the internal microstructure c) 200x magnification.

The coating surface is covered with individual fused-on spherical powder particles, caused by the manufacturing process and result of the impact effect of the powder particles on the coating surface. In its initial state, the coating surface has an average surface roughness Ra of 5.85 µm and an average roughness depth Rz of 27.91 µm. The coating thickness varies between 280 – 355 µm.

3.2. Influence of energy per unit length on the achievable surface roughness

The initial parameter study conducted in this work aims to investigate the influence of the energy per unit length E_{Dis} on the achievable surface quality by varying the laser power P_l between 175 – 350 W and the scanning speed v_s between 100 – 400 mm/s to identify the process parameter thresholds. With these parameter combinations, E_{Dis} is varying between 0.4 – 3.5 kJ/m. The parameter study was performed with a constant hatch distance d_{hatch} of 75 µm, resulting in a track overlap of 91.4%. The complete experimental plan is given in Table 2.

Table 2 Variable laser parameters of test series 1

Test Field number	Laser power P_l [W]	Scanning speed v_s [mm/s]	Energy per unit length E_{dis} [kJ/m]	Energy density ED [J/mm²]
1 - 6	175; 210; 245; 280; 315; 350	100	1.8; 2.1; 2.5; 2.8; 3.2; 3.5	23.3; 28.0; 32.7; 37.3; 42.0; 46.7
7 - 12	175; 210; 245; 280; 315; 350	200	0.9; 1.1; 1.2; 1.4; 1.6; 1.8	11.7; 14.0; 16.3; 18.7; 21.0; 23.3
13 - 18	175; 210; 245; 280; 315; 350	300	0.6; 0.7; 0.8; 0.9; 1.1; 1.2	7.8; 9.3; 10.9; 12.4; 14.0; 15.6
19 - 24	175; 210; 245; 280; 315; 350	400	0.4; 0.5; 0.6; 0.7; 0.8; 0.9	5.8; 7.0; 8.2; 9.3; 10.5; 11.7

Independent from the applied laser power, polishing with a scanning speed v_s of 100 mm/s results in a delamination of the thermal sprayed coating, see Fig. 3. At higher scanning speeds three process regimes exist. With a laser power of 175 W in combination with a scanning speed of 400 mm/s (E_{Dis} = 0.4 kJ/m) only local micro remeltings of the surface structure happens. Most of the surface is almost unaffected. With rising energy per unit length the proportion of remelted surface structures increases. For a full remelting of the initial surface at least 0.6 kJ/m are necessary. Further rising energy per unit length results in a darker surface appearance and higher gloss level.

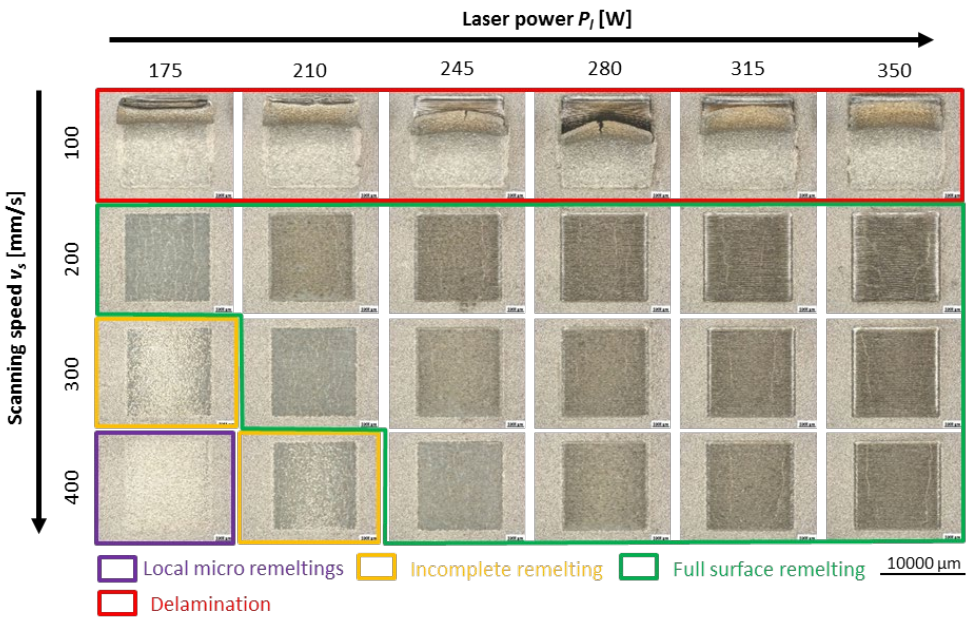

Fig. 3 Process regimes at varying laser power P_l and scanning speed v_s at laser polishing, analysed by microscopic images with a 8-fold magnification

Laser polishing with E_{Dis} = 0.4 kJ/m causes almost no change of the surface topography. Only small surface elevations are flattened, see Fig. 4 a). With an energy per unit length of 0.5 kJ/m an increasing amount of the initial structures are remolten and flattened, but the long-wavelength surface structures are still present due to incomplete surface remelting. If a complete surface melting is achieved, material accumulations at the starting and end position of the scanning vectors with a height of up to 30 µm occurs. Perpendicular to the scanning directions a continuous crack emerges. Using a energy per unit length of 1.8 kJ/m, the central area of the polishing field is cracking and delamination of the Hastelloy® coating occurs (Fig. 4 d)).

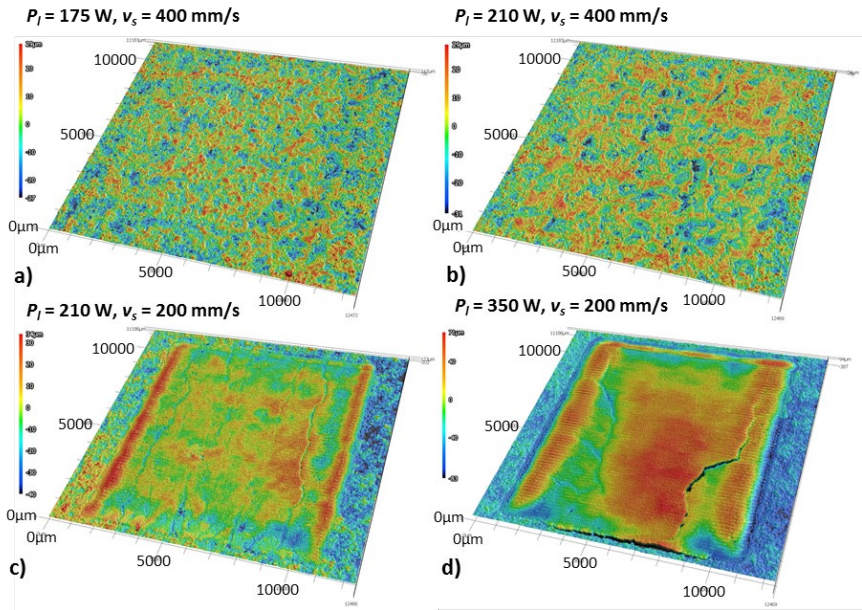

Fig. 4 Surface topography depending on the applied energy per unit length E_{Dis}, measured by laser scanning microscope

A more detailed view on the residual surface structures depending on the applied energy per unit length is given in Fig. 5. With E_{Dis} = 0.9 kJ/m, within the completely remolten surface cracks can be observed. With further increasing energy input per unit length, the width of the remelting pathways rises and causes linear surface structures, see Fig. 5 a) with E_{Dis} 1.8 kJ/m. While the short structure waviness of the initial surface is flattened already with less energy input, the larger surface structures and waviness can be continuously further reduced with steadily increasing E_{Dis}. Too high energy input per unit length causes a surface linear structuring by the remelting paths.

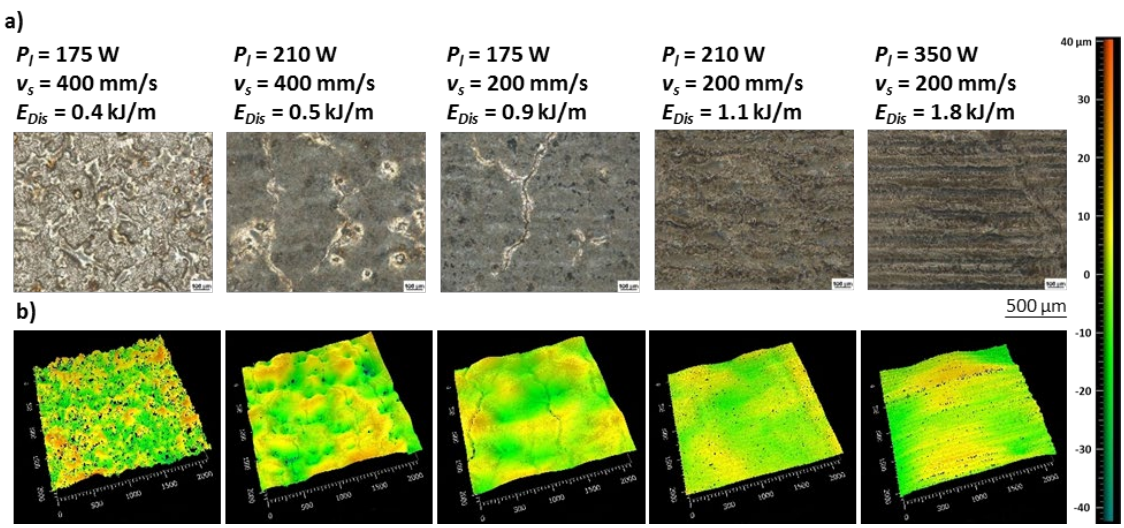

Fig. 5 Residual microstructures depending on the energy per input length E_{Dis},: a) microscopic images with a 100-fold magnification, b) white light interferometer images with a 10-fold magnification

The linear measured arithmetic surface roughness Ra is steady decreasing with rising energy per unit length up to its minimum of Ra = 1.11 µm, which is achieved at E_{Dis} = 0.8 kJ/m in combination with a scanning speed of 300 mm/s, see Figure 3. With further increasing E_{Dis}, the roughness is slightly increasing Ra = 2.35 µm almost independent from the applied scanning speed, due to surface structuring, shown in Figure 2. The same dependencies and surface roughness minimum occurs at the roughness depth Rz.

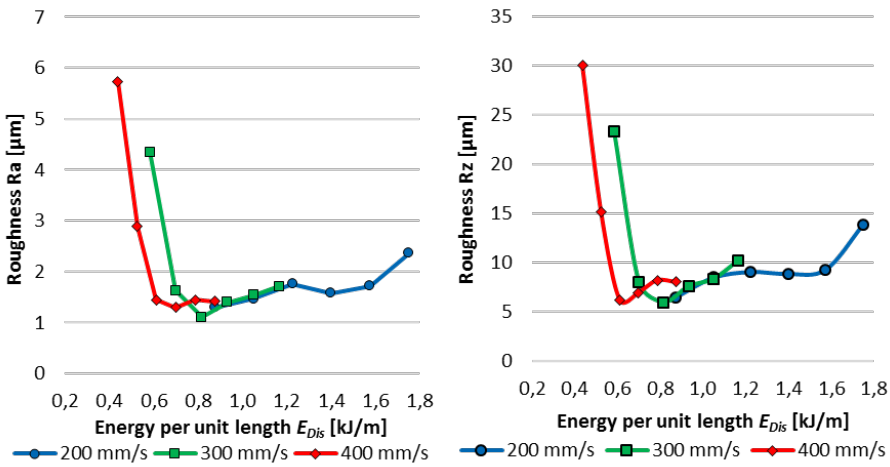

Fig. 6 Arithmetic roughness Ra and arithmetic roughness depth Rz depending on the applied energy per unit length E_{Dis} and used scanning speed v_s

3.3. Influence of track overlap and energy density on the achievable surface roughness

The second test series conducted in this work analyses the influence of the track overlap *TO* and the varying energy density *ED* on the achievable surface roughness at variable laser beam intensities. Hereto the hatch distance d_{hatch} is varied from 92.5 µm to 40.0 µm. The resulting track overlap is changing from 89.4% to 95.4%. This study is performed with a constant energy per unit length of 0.8 kJ/m, which was found to be best at study one. In order to investigate the influence of different scanning speeds and beam intensities on the resulting surface properties, the scanning speed is changed from 200 – 700 mm/s at adapted laser powers of 163 – 572 W , resulting in beam intensities between 0.27 – 0,96 kW/mm². The full experimental plan is given in Table 3.

Table 3 Variable laser parameter of test series 2

Test Field number	Laser power P_l [W]	Beam intensity I [kW/mm²]	Scanning speed v_s [mm/s]	Hatch distance d_{hatch} [µm]	Track overlap *TO* [%]	Energy density *ED* [J/mm²]
1 - 6	163; 245; 327; 408; 490; 572	0.27; 0.41; 0.55; 0.69; 0.82; 0.96	200; 300; 400; 500; 600; 700	92.5	89.4%	8.8
7 - 12	163; 245; 327; 408; 490; 572	0.27; 0.41; 0.55; 0.69; 0.82; 0.96	200; 300; 400; 500; 600; 700	75.0	91.4%	10.9
13 - 18	163; 245; 327; 408; 490; 572	0.27; 0.41; 0.55; 0.69; 0.82; 0.96	200; 300; 400; 500; 600; 700	57.5	93.4%	14.2
19 - 24	163; 245; 327; 408; 490; 572	0.27; 0.41; 0.55; 0.69; 0.82; 0.96	200; 300; 400; 500; 600; 700	40.0	95.4%	20.4

Laser polishing with increasing beam intensity at a constant energy per unit length reveals a rising surface structuring by the individual scanning lines, see Fig. 7.

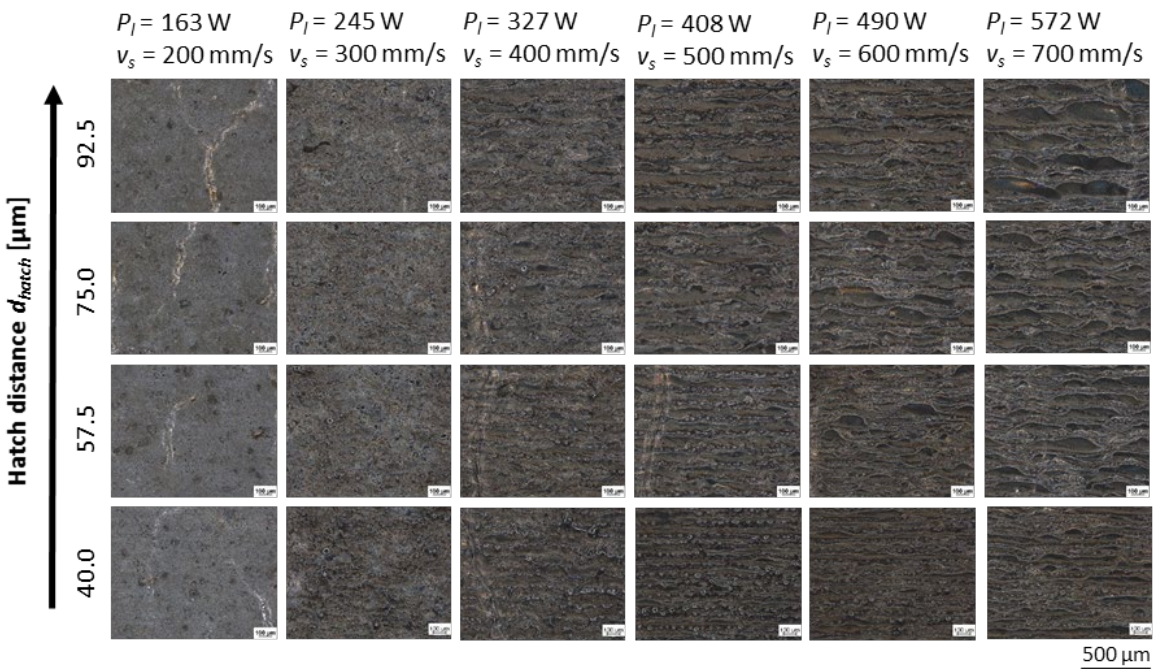

Fig. 7 Influence of beam intensity *I* and hatch distance d_{hatch} at a constant energy per unit length E_{Dis} of 0.8 kJ/m on the resulting surface characteristics

While at low beam intensities of less than 0.41 kW/mm² no linear hatchings can be observed on the surface and a homogeneous surface characteristics exists, the width of the visible linear scanning tracks are increasing with rising laser power. A decreasing hatch distance results in a clearly visible higher track overlap of the created remelting paths. Over all, the surface appearance is changing between a scanning speed of 200 mm/s and 300 mm/s into a darker surface.

Within this study, the achievable surface roughness Ra is varying from 1.17 – 1.10 µm and 10.2 – 5.8 µm in Rz, see Fig. 8. The applied beam intensity *I* and used scanning speed v_s has no effect on the resulting surface roughness. Moreover, a significant influence of the track overlap on the resulting surface quality cannot be observed. The overall best surface quality is achieved with a scanning speed of 300 mm/s in combination with a track overlap of 91.4%. The same applies for the roughness depth Rz.

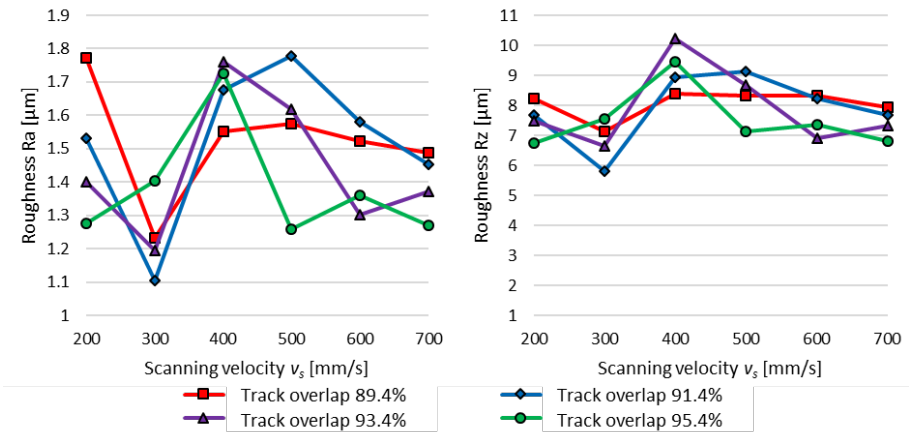

Fig. 8 Achievable surface roughness depending on the scanning speed v_s and applied track overlap *TO* with a constant energy per unit length E_{Dis} of 0.8 kJ/m

The lowest residual waviness is achieved with a scanning speed of 300 mm/s. At the highest beam intensity and scanning speed, visible linear structures from the individual scanning pathes are created. With reduced hatch distance (higher track overlap) the process introduced linear structures can be reduced, see Fig. 9.

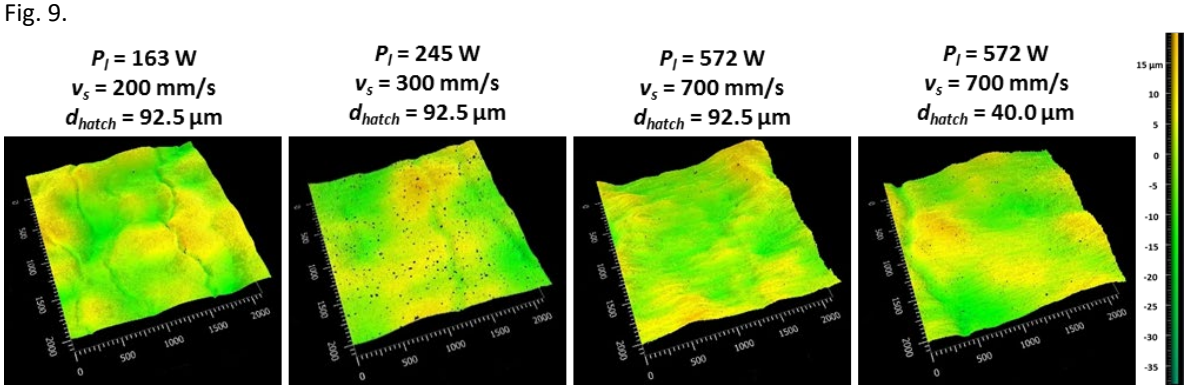

Fig. 9 Surface topography depending on the beam intensity *I* and hatch distance d_{hatch} at a constant energy per unit length E_{Dis} of 0.8 kJ/m

3.4. Process limitations due to delamination

Even with insufficient low energy per unit length of E_{Dis} = 0.4 kJ/m, vertical cracks at the surface near area exist, see cross section a) of Fig. 10. At the connection area to the substrate underneath, small cracks can be observed, too. With increasing laser power delamination of the coating in combination with vertical consistent cracks occurs, Fig. 10 b). With further increasing E_{Dis} due to a reduced scanning speed wide cracks are formed. When observing the surface structures at the bonding area, a clear visible shrinkage of the coating in the opposite direction to the continuous wide crack on the left hand side can be detected, Fig. 10 c).

Main reason for that might be an insufficient bonding to the thermal sprayed coating to the substrate. Due to the introduced local high process temperatures at the coating surface with big temperature gradients into the depth in combination with different thermal expansion coefficients of the Hastelloy® coating and the

substrate, made of low alloyed steel, internal stress occurs resulting in material failure.

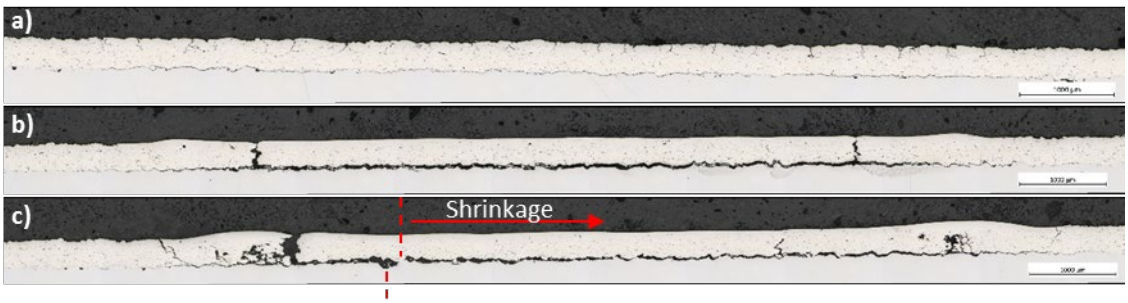

Fig. 10 Cross section of the polishing fields; a) 175 W, 400 mm/s, E_{Dis} = 0.4 kJ/m; b) 350 W, 400 mm/s, E_{Dis} = 0.9 kJ/m; c) 350 W, 200 mm/s, E_{Dis} = 1.8 kJ/m

4. Conclusion and outlook

Laser polishing with a single polishing pass achieves a roughness reduction of up to 81% to a arithmetic roughness Ra of 1.11 µm at an energy per unit length of 0.8 kJ/m. A completely dens surface, without surface open porosity is created. With higher applied energy densities material accumulations at the scanning vector beginning and end occurs. The track overlap varied in the range of 85.4 – 95.4% has no significant influence on the achievable surface quality. When applying the same energy per unit length, with increasing beam intensity linear surface structuring caused from the individual laser paths is increasing, which can be reduced with a higher track overlap. However, delamination and the formation of cracks occurring even at lowest remelting depths is a main drawback.

For the future work, a homogeneous pre- heating of the specimens will be applied. It aims to reduce the temperature gradients within the coating layer and in relation to the substrate underneath in order to minimize the creation of internal stresses due to the very fast material re-melting and solidification by the laser polishing process. Additionally the further roughness reduction ability by multiple laser polishing passes will be investigated.

Acknowledgements

The authors acknowledge support by the Federal Ministry of Economics and Technology German, program “ZIM” (Zentrales Innovationsprogramm Mittelstand) for the financial support of the project LaVets.

References

C. Huang, J. Wang, J. Yan, L. Liao, 2023. Evaluation of corrosion and wear performance of Fe-based coating and hastelloy C276 in H2S environment on 304 stainless steel substrate. Colloids and Surfaces A: Physicochemical and Engineering Aspects Volume 674, https://doi.org/10.1016/j.colsurfa.2023.131871

E.V. Bordatchev, A.M.K. Hafiz, 2014. Performance of laser polishing in finishing of metallic surfaces. The International Journal of Advanced Manufacturing Technology 73, p.35-52, DOI 10.1007/s00170-014-5761-3

G. Singh, V. Aggarwal, S. Singh, B. Singh, S. Sharma, J. Singh, C. Li, G. Krolczyk, A. Kumar, S. M. Eldin, 2023. “Performance investigations for sustainability assessment of Hastelloy C-276 under different machining enviroments. Heliyon 9, https://doi.org/10.1016/j.heliyon.2023.e13933

H. Herman, S. Sampath, R. McCune, 2000. Thermal Spray: Current Status and Future Trends. MRS Bull., 25 (7) p.17

H.S. Ni, X.H. Liu, X.C. Chang, W.L. Hou, W. Liu, J.Q. Wang, 2009. High performance amorphous steel coating prepared by HVOF thermal spraying. Alloys and Compounds Volume 467, Issues 1-2, p. 163-167, https://doi.org/10.1016/j.jallcom.2007.11.133

M.K. Srinath, J. Nagendra, 2022. Post-processing parameter optimization to enhance the surface finish of HVOF-developed coatings. Multiscale and Multidisciplinary Modeling, Expriments and Design, 5:255-267, https://doi.org/10.1007/s41939-022-00116-x